ELSEVIER

Journal of Alloys and Compounds 446–447 (2007) 469–473

Journal of ALLOYS AND COMPOUNDS

www.elsevier.com/locate/jallcom

Point defect dynamics in sodium aluminum hydrides—A combined quasielastic neutron scattering and density functional theory study

Q. Shi [a,b], J. Voss [a,c], H.S. Jacobsen [a,b], K. Lefmann [a], M. Zamponi [d], T. Vegge [a,*]

[a] Materials Research Department, Risø National Laboratory, Technical University of Denmark, DK-4000 Roskilde, Denmark
[b] Niels Bohr Institute, University of Copenhagen, DK-2100 Copenhagen Ø, Denmark
[c] Centre for Atomic-scale Materials Design and Department of Physics, Technical University of Denmark, DK-2800 Kgs. Lyngby, Denmark
[d] Institut für Festkörperforschung, Forschungszentrum Jülich, D-52425 Jülich, Germany

Received 6 October 2006; received in revised form 30 March 2007; accepted 2 April 2007
Available online 12 April 2007

Abstract

Understanding the catalytic role of titanium-based additives on the reversible hydrogenation of complex metal hydrides is an essential step towards developing hydrogen storage materials for the transport sector. Improved bulk diffusion of hydrogen is one of the proposed catalytic effects, and here we study hydrogen dynamics in undoped and $TiCl_3$-doped samples of $NaAlH_4$ and Na_3AlH_6 using a combination of density functional theory calculations and quasielastic neutron scattering. Hydrogen dynamics is found to be limited and mediated by hydrogen vacancies in both alanate phases, requiring an activation in excess of 0.3 eV. Even at 390 K, less than 1% of the hydrogen in $NaAlH_4$ performs long range diffusion, and only localized hydrogen dynamics is observed in Na_3AlH_6. The effect of the $TiCl_3$ dopant on hydrogen bulk diffusion is found to be negligible.

Keywords: Hydrogen storage materials; High-energy ball milling; Neutron scattering; Electronic band structure; Localized hydrogen motion

1. Introduction

Titanium based dopants have been found to catalyze the decomposition and regeneration of $NaAlH_4$ [1], but the physical explanation has remained elusive. A number of different models have been proposed to describe the catalytic effect of titanium [2,3], one suggesting improved hydrogen diffusion from bulk substitution of titanium for aluminum or sodium [4].

Hydrogen dynamics between interstitial sites in Laves phase materials [5] can be investigated using quasielastic neutron scattering (QENS), but to describe $NaAlH_4$ and Na_3AlH_6, with and without a $TiCl_3$ precursor, density functional theory calculations (DFT) are also needed.

We find hydrogen diffusion to be mediated by hydrogen vacancies and to require significant thermal activation. Furthermore, significantly improved hydrogen diffusion by bulk substitution of Ti at Na or Al-sites is not observed.

2. Calculational setup

The electronic structure is calculated using density functional theory [6] in the DACAPO plane wave basis set implementation [7]. The ion cores are described by ultrasoft pseudopotentials [8], and the exchange and correlation effects are described by the PW91 functional [9]. The Kohn-Sham wavefunctions are expanded in a plane wave basis set with a cutoff energy of 25 Ry (for the density grid a cutoff of 45 Ry is used). The wave functions are sampled on a *k*-point mesh of spacing ~ 0.3 Å^{-1} in all three directions.

The optimum crystal structure at zero temperature is obtained by iterative relaxation of unit cell parameters and atomic coordinates. For the calculation of formation and activation energies, we use computational $(2 \times 2 \times 1)$ supercells for the $NaAlH_4$ and Na_3AlH_6 systems. Vacancies are created by removing an atom from the supercell and re-relaxing the atomic coordinates; two such neighboring vacancy configurations are then considered as initial and final states of a vacancy mediated diffusion process.

The rate τ^{-1} of a thermally activated process decreases exponentially with the ratio of the activation energy E_{act} to tem-

---

[*] Corresponding author. Tel.: +45 4677 5818; fax: +45 4677 5758.
E-mail address: tejs.vegge@risoe.dk (T. Vegge).

0925-8388/$ – see front matter © 2007 Elsevier B.V. All rights reserved.
doi:10.1016/j.jallcom.2007.04.041

perature $k_B T$. Within harmonic transition state theory (hTST) [10], the pre-exponential factor depends only on the eigenfrequencies of the initial and transition states; hTST has previously been shown to be able to describe complex systems and elevated temperatures [11,12]. We use the nudged elastic band (NEB) [13] path technique to accurately locate the transition states for the hydrogen dynamics.

3. Experimental methods and diffusion models

Four different samples were prepared and analyzed. $NaAlH_4$ (Sigma–Aldrich, 90%) and the catalyst precursor $TiCl_3$ (Alfa Aesar, $TiCl_3 \cdot$ (1/3)$AlCl_3$, purity 76–78% $TiCl_3$) were used as received in powder form. The undoped Na_3AlH_6 sample was synthesized by energetic ball-milling of stoichiometric mixtures of NaH (Sigma–Aldrich, 95%) and $NaAlH_4$, as proposed by Huot et al. [14], for 5 h. The doped Na_3AlH_6 sample was prepared by 4.5 h ball-milling of the mixture and a subsequent half hour ball-milling with 4 mol% $TiCl_3$ additive. To eliminate potential crystallite size effects [15], the undoped and doped $NaAlH_4$ samples were ball-milled in the same way as Na_3AlH_6.

All materials handling was performed within an argon-filled glove box, and all samples were characterized with X-ray powder diffraction, see Refs. [16,17].

The QENS experiments were performed on the high-resolution backscattering spectrometer (BSS) located at the Forschungszentrum Jülich. The samples were loaded in flat 0.1 mm × 30.0 mm × 40.0 mm Al containers and oriented close to 45° with respect to the incident beam. The spectra were recorded by ten detectors which correspond to a range of scattering vectors of $q = 0.16$–$1.87\,\text{Å}^{-1}$. The measured neutron scattering intensity in the experiments can be expressed as

$$S_{\text{inc}}^{\text{tot}}(q,\omega) = R(q,\omega) \otimes (B_0\delta(\omega) + B_1 L_0(\omega,\Gamma)) + C_{\text{back}}, \quad (1)$$

in which $B_0\delta(\omega)$ is the elastic peak, $B_1 L_0(\omega,\Gamma)$ the quasielastic lorentzian, and C_{back} is the constant background term. The resolution function $R(q,\omega)$ is determined from the measured QENS spectra of each sample at low temperature ($T = 30$ K) [16].

The finite steps of diffusing atoms in lattices are taken into account by the Chudley-Elliott (CE) model [18]. For long range diffusion of atoms, the quasielastic line broadening, Γ, is given for large q by

$$\Gamma(q) = \frac{6D}{L^2}\left(1 - \frac{\sin qL}{qL}\right), \quad (2)$$

with the hydrogen jump length L and a hydrogen diffusion constant $D = L^2/(6\tau)$.

The CE model assumes a random-walk of the diffusing species [18]. For the vacancy mediated diffusion observed here, the motion of the vacancy is a random walk, while the involved atomic jumps are correlated. In a zero-order approximation, i.e. one atomic jump per vacancy diffusion step, the only effect is a rescaling of τ [19], which will cause negligible errors in the estimated activation energies [17].

Localized hydrogen dynamics causes q-independent quasielastic broadening for large scattering vectors [20,21], yet lower diffusion rates may result in a q-dependent broadening at lower q (see Appendix A).

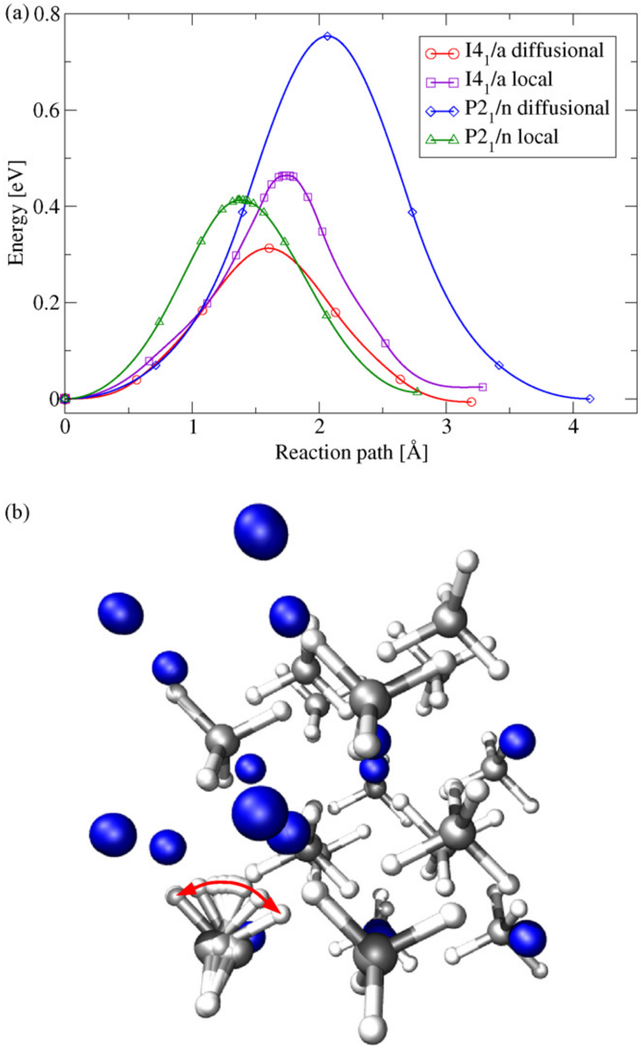

Fig. 1. The calculated minimum energy diffusion path for localized hydrogen motion in undoped $NaAlH_4$(a) (representing colors: sodium: blue; aluminum: gray; hydrogen: white) and the calculated activation energies for localized H dynamics and long range H diffusion in $NaAlH_4$ and Na_3AlH_6(b). (For interpretation of the references to colour in this figure legend, the reader is referred to the web version of the article.)

In addition to fitting the QENS data to the CE model (Eq. 2), we estimate the volume accessible to the diffusing hydrogen (vacancy) from the ratio of elastic to total scattering intensity, the so-called elastic incoherent structure factor (EISF) [22]. The EISF is proportional to the absolute square of the Fourier transform of the accessible volume [23]. The diffusing species are constricted to two perpendicular planes corresponding to the four possible jumps of a vacancy in a $(AlH_5)^{2-}$ complex (see Fig. 1 (a)), assuming a radially symmetric probability density in the planes. Approximating the powder average by a three-point integration over the polar angle θ with vanishing $\sin(\theta)$ at the end points, the normalized EISF A_0 can be written as

$$A_0(q) = \frac{1}{4}\left|\int_0^{\infty} \mathrm{d}r\rho(r)r[j_0(qr) + 1]\right|^2 \quad (3)$$

j_0 is the Bessel function of order zero. We estimate the radial probability density $\rho(r)$ by a least squares fit of the experimental data for the EISF to Eq. (3).

4. Results from neutron scattering

The samples were subjected to elastic temperature scans to identify potential transitions temperatures, where scattering intensity is transferred from the elastic to the inelastic regions.

For doped $NaAlH_4$, no drop in elastic scattering intensity – except for the Debye-Waller factor – is seen for temperatures up to 315 K (Fig. 2); a similar scan for undoped $NaAlH_4$ up to 412 K indicated no significant hydrogen dynamics below ∼ 350 K [16].

For doped Na_3AlH_6, a small and gradual transfer is observed at temperatures above ∼ 250 K and similarly in a $\leq$ 350 K scan for undoped Na_3AlH_6 [17].

Quasielastic scans were performed on $NaAlH_4$ at 30, 315, 390 K and 30, 315 K for doped $NaAlH_4$ [16]. For Na_3AlH_6, the scans were performed at 30, 150, 250, 350, 390 K for the undoped sample and 30, 250, 300, 350 K for the doped sample (see Ref. [17]). Due to the high equilibrium pressure of Ti-doped samples [24], we were not able to go to higher temperatures.

The QENS data for $NaAlH_4$ revealed that neither the doped nor the undoped samples displayed any quasielastic broadening at temperatures $\leq$ 315 K. In fact, only approx. half a percent of the hydrogen was mobile in the undoped sample at 390 K.

For Na_3AlH_6, no quasielastic broadening was observed below 350 K, and even at this temperature only the doped sample displayed a significant amount of mobile hydrogen (2%). At 390 K, the undoped Na_3AlH_6 sample did display significant broadening (13% mobile hydrogen) and a clear CE-type (Eq. 2) q-dependence, see Ref. [17].

Inverse jump rates and jump lengths for the mobile hydrogen atoms (see Fig. 1 and Table 1) were obtained by fitting QENS data to the CE model (2) using prefactors from the DFT calculations, since reliable QENS data was only available at one temperature for each sample.

A least squares fit of the EISF (see Fig. 3) to Eq. (3) for undoped and doped Na_3AlH_6 yields jump lengths around 2.8 Å (see Fig. 4), in good agreement with the Chudley-Elliott fit and the DFT results for localized hydrogen dynamics [17]. Large peaks at $r = 0$ account for immobile hydrogen. In order to increase the resolution of $\rho(r)$, the experimental values for the EISF have been interpolated with splines. The EISF for undoped $NaAlH_4$ at 390 K (see Fig. 3) does not display a q-dependence within the given experimental resolution, suggesting a non-localized process.

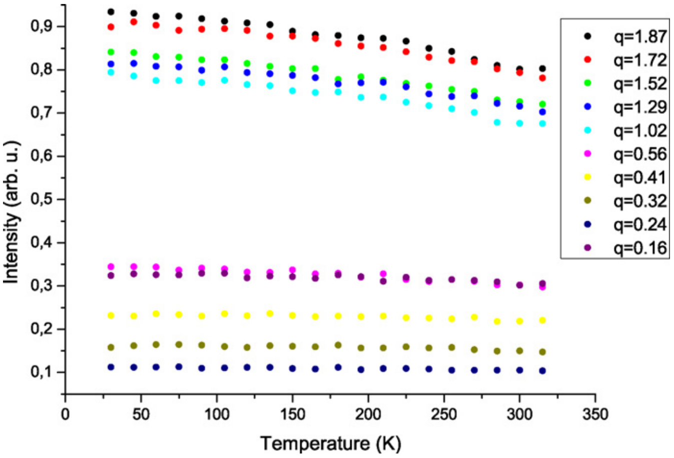

Fig. 2. Elastic temperature scan for $NaAlH_4$ doped with 4 mol% $TiCl_3$.

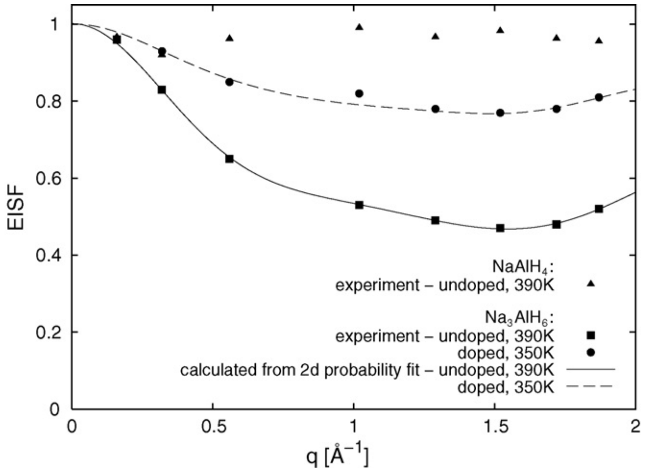

Fig. 3. Elastic incoherent structure factor for $NaAlH_4$ and Na_3AlH_6.

Table 1

The calculational results for Local dynamics and long range Diffusion are labeled DFT_L and DFT_D, respectively. The QENS values rely on the DFT prefactors to determine E_{act}

	$NaAlH_4$				Na_3AlH_6			
	T (K)	$\tau^{-1}(T)$ (GHz)	L_{jump} (Å)	E_{act} (eV)	T (K)	$\tau^{-1}(T)$ (GHz)	L_{jump} (Å)	E_{act} (eV)
Undoped samples								
QENS	390	0.4	∼2.6	0.39	390	0.4	2.80	0.37
DFT_L		0.09	2.55	0.44		0.1	2.50	0.41
DFT_D		5	2.78	≥0.31		9×10^{-6}	3.08	≥0.75
Titanium doped samples								
QENS	315	<0.25[a]			350	0.8	2.8	0.31
DFT_L				No well-defined path;H trapped by Ti				
DFT_D			H trapped by Ti			0.1	2.80	≥0.36

[a] Derived from the instrumental resolution.

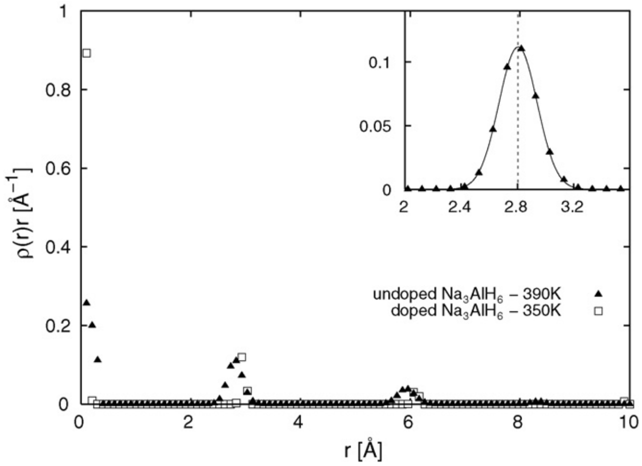

Fig. 4. Radial probabilty densities for diffusing species in undoped and doped Na_3AlH_6 (*inset*: Gaussian fit to first peak at $r = 2.81 \pm 0.14$ Å).

5. Calculations results

In order to clearly identify the dynamic events observed in the QENS data, we have calculated the prefactors and activation energies for long range H diffusion and localized H dynamics using DFT. We find hydrogen diffusion to be vacancy mediated due to high formation energies of interstitials. For undoped $NaAlH_4$, the formation energy for a hydrogen vacancy is 1.61 eV while the cost for an interstitial is 2.40 eV (for Na_3AlH_6 the energies are 1.54 and 2.42 eV, respectively [17]).

In undoped $NaAlH_4$, diffusion from an $(AlH_4)^-$ tetrahedron to a faulted AlH_3 complex is found to have the lowest activation energy of E_{act}=0.31 eV (see Fig. 1b). The barrier for localized motion (see Fig. 1a) in the same AlH_3 complex is 0.44 eV. These findings agree with the 0.39 eV obtained from the QENS data (Table 1) and the EISF results.

In undoped Na_3AlH_6, long range H diffusion is limited ($E_{act} \geq 0.75$ eV), while the barrier for localized dynamics, where the vacancy remains bound to the same Al-atom is significantly lower: 0.41 eV (see Fig. 1b). The QENS barrier is found to be 0.37 eV, in clear support of the localized dynamics observed in the EISF.

To calculate the potential effect of bulk substituted titanium on the hydrogen dynamics, the Al-sites were used since they are energetically preferred over Na-sites for both $NaAlH_4$ [25] and Na_3AlH_6 [17]. For an insignificant fraction of the hydrogen atoms in doped Na_3AlH_6 (< 1% for doping with 4 mol% $TiCl_3$), the activation energy for long range diffusion could be lowered to 0.36 eV (see Table 1). For doped $NaAlH_4$, H is trapped by Ti for Ti–H distances up to at least ∼7 Å. Neither case would yield significantly improved hydrogen dynamics.

6. Discussion

The barrier for long range hydrogen diffusion in $NaAlH_4$ was found to be lower than the barrier for localized hydrogen dynamics, whereas the opposite is observed for Na_3AlH_6, effectively excluding long range diffusion in this alanate.

Excellent agreement between the QENS and DFT data shows that a limited amount of hydrogen diffusion is observed in $NaAlH_4$, whereas only localized hydrogen dynamics is found in Na_3AlH_6. In both cases, high temperatures are needed and the addition of a $TiCl_3$ catalyst was found to have a limited effect on the bulk hydrogen dynamics.

Acknowledgements

The authors acknowledge financial support by the NABIIT program and the DANSCATT center funded by the Danish Research Council, and the European Commission under the 6th Framework through the Key Action: Strengthening the European Research Area, Research Infrastructures, Contract no: RII3-CT-2003-505925. The authors would like to acknowledge the Danish Center for Scientific Computing (DCSC) for supercomputer access.

Appendix A. Quasielastic broadening in the case of low diffusion rates

In Singwi and Sjölander's model for diffusive motion [20], the diffusing species oscillate around their equilibrium position for a mean time τ_{osc} and then diffuse continuously for a mean time τ_{diff}. The effective diffusion constant is $D \approx L^2/(6(\tau_{diff} + \tau_{osc}))$ (L is the jump length). For $\tau_{diff} \gg \tau_{osc}$, the broadening of the differential scattering cross-section is dominated by continuous diffusion, displaying a q^2-dependence [20]. For $\tau_{diff} \ll \tau_{osc}$, the shape of the differential scattering cross-section is a Lorentzian, the width of which becomes q-independent for $q^2 D\tau_{osc} \gg 1$. We assume this inequality to be fulfilled, but we do not restrict τ_{diff} to be much smaller than τ_{osc}. With inverse diffusion rates of the order of 1 ns for localized events in Na_3AlH_6 and broadenings of the order of 1 μeV, we have $q^2 D\tau_{osc} \gg 1 \sim \omega^2\tau_{diff}^2$. Using Eqs. (15a), (15b) and (17) from Ref. [20], we obtain the following simplified expression for half-width at half maximum of the differential scattering cross-section:

$$\Delta\omega = \frac{q^2 D(\tau_{diff} + \tau_{osc})}{\sqrt{\tau_{osc}^2 q^4 D^2 (\tau_{diff} + \tau_{osc})^2 + 2\tau_{diff}\tau_{osc}}}. \qquad \text{(A.1)}$$

In order to approach the asymptotic limit τ_{osc}^{-1} of (A.1), the condition $q^2 L^2 \gg 6\sqrt{2\tau_{diff}/\tau_{osc}}$ must be fulfilled. A q-dependent broadening for larger wave vectors could therefore be explained by lower diffusion rates τ_{diff}^{-1}.

References

[1] B. Bogdanović, M. Schwickardi, J. Alloys Compd. 253/254 (1997) 1.
[2] F. Schüth, B. Bogdanović, M. Felderhoff, Chem. Commun. (2004) 2249.
[3] T. Vegge, Phys. Chem. Chem. Phys. 8 (2006) 4853.
[4] D. Sun, T. Kiyobayashi, H.T. Takeshita, N. Kuriyama, C.M. Jensen, J. Alloys Compd. 337 (2002) L8.
[5] D.J. Bull, D.K. Ross, J. Alloys Compd. 293–295 (1999) 296.
[6] W. Kohn, L.J. Sham, Phys. Rev. 140 (1965) A1133.
[7] B. Hammer, L.B. Hansen, J.K. Nørskov, Phys. Rev. B 59 (1999) 7413 (Dacapo pseudopotential code) http://www.fysik.dtu.dk/campos.
[8] D. Vanderbilt, Phys. Rev. B 41 (1990) R7892.

[9] J.P. Perdew, J.A. Chevary, S.H. Vosko, K.A. Jackson, M.R. Pederson, D.J. Singh, C. Fiolhais, Phys. Rev. B 46 (1992) 6671.

[10] P. Hänggi, P. Talkner, M. Borkovec, Rev. Mod. Phys. 62 (1990) 251.

[11] T. Vegge, T. Rasmussen, T. Leffers, O.B. Pedersen, K.W. Jacobsen, Phys. Rev. Lett. 85 (2000) 3866.

[12] T. Vegge, Phys. Rev. B 70 (2004) 034512.

[13] H. Jónsson, G. Mills, K.W. Jacobsen, B.J. Berne, G. Ciccoti, D.F. Coker, in: Classical and Quantum Dynamics in Condensed Phase Simulations, World Scientific, Singapore, 1998.

[14] J. Huot, S. Boily, V. Güther, R. Schulz, J. Alloys Compd. 283 (1999) 304.

[15] A. Andreasen, T. Vegge, A.S. Pedersen, J. Solid. State Chem. 178 (2005) 3672.

[16] T. Vegge, Q. Shi, J. Voss, H.S. Jacobsen, M. Zamponi, K. Lefmann, submitted for publication.

[17] J. Voss, Q. Shi, H.S. Jacobsen, M. Zamponi, K. Lefmann, T. Vegge, J. Phys. Chem. B 111 (2007) 3886.

[18] C.T. Chudley, R.J. Elliott, Proc. Phys. Soc. 77 (1961) 353.

[19] O. Bender, K. Schroeder, Phys. Rev. B 19 (1979) 3399.

[20] K.S. Singwi, A. Sjölander, Phys. Rev. 119 (1960) 863.

[21] P.L. Hall, D.K. Ross, Mol. Phys. 42 (1981) 673.

[22] M. Bée, Physica B 182 (1992) 323.

[23] M. Bée, Quasielastic Neutron Scattering, Hilger, Bristol, 1988.

[24] B. Bogdanović, R.A. Brand, A. Marjanović, M. Schwickardi, J. Tölle, J. Alloys Compd. 302 (2000) 36.

[25] O.M. Løvvik, S.M. Opalka, Appl. Phys. Lett. 88 (2006) 161917.